

## Numerical Modelling of Biomass Grate Furnaces

Robert Scharler<sup>1</sup>, Ingwald Obernberger<sup>1,2</sup>

<sup>1</sup>Institute of Chemical Engineering Fundamentals and Plant Engineering,  
Technical University Graz, A-8010 Graz, Austria

email: scharler@glvt.tu-graz.ac.at

<sup>2</sup>BIOS – Bioenergy Systems, Sandgasse 47/13, A-8010 Graz, Austria

### Abstract

Computational Fluid Dynamics (CFD) is increasingly being used for the optimisation of industrial coal furnaces and gas burners. Due to the high complexity of heterogeneous combustion of fixed or moving biomass fuel beds, only few research projects have so far dealt with the introduction of CFD as a cost-efficient tool in the optimisation of biomass grate furnaces. The present work covers the application and evaluation of the commercial CFD code FLUENT™ focusing on its capability of treating the specific problem of modelling biomass grate-furnaces and the necessity of implementing additional sub-models. A case study regarding the optimisation of the geometry of the combustion chambers and secondary air nozzles was performed. The major goal of CFD modelling is a techno-economic optimisation of the furnace (reduction of furnace volume, optimisation of the mixing of flue gas and air, reduction of erosion by fly ash as well as of emissions by primary measures).

Simulation results for a pilot plant equipped with a travelling grate furnace (nominal boiler capacity 440 kW<sub>th</sub>) and for a newly designed plant, also equipped with a travelling grate (nominal boiler capacity 550 kW<sub>th</sub>), are presented. An empirically derived model was used for the calculation of mass and energy fluxes entering from the fuel bed on the grate into the gas phase, thus forming the boundary conditions for subsequent CFD calculations. For the modelling of turbulent reacting flows in the furnace, the Realizable k-ε Turbulence Model, the Discrete Ordinates Radiation Model and a modified Eddy Dissipation Combustion Model with a 3-step global reaction mechanism considering 6 species (C<sub>m</sub>H<sub>n</sub>, H<sub>2</sub>O, H<sub>2</sub>, CO, CO<sub>2</sub>, O<sub>2</sub>) were applied. The parameters of the empirical model describing the release of energy and mass from the fuel bed will be determined by applying a specially developed FT-IR measurement technique that makes hot gas in-situ measurements of CO, CO<sub>2</sub>, H<sub>2</sub>O and CH<sub>4</sub> in the furnace possible. Plausibility of results achieved by CFD calculations is checked by test runs at the furnace simulated.

The results of the CFD calculations revealed a considerable potential for the optimisation of furnace geometry and secondary air nozzles regarding the mixing of fuel and air. Even with isothermal flow calculations the volume of the furnace geometry can be minimised by visualisation of dead zones. Moreover, erosion can be reduced by estimation of erosion rates with a particle tracing procedure. The Eddy Dissipation Model used is reasonably accurate for most industrial flow problems but cannot properly describe strong coupling between turbulence and multi-step chemistry (e.g. NO<sub>x</sub> calculations). Therefore, an advanced Eddy Dissipation Concept (e.g. for NO<sub>x</sub> calculations with a post-processor) is being implemented. Taking the results already achieved into consideration it can be stated that CFD calculations generally represent an efficient tool for the techno-economic optimisation of biomass fixed-bed combustion systems.

### Keywords

CFD modelling, biomass, combustion, Eddy Dissipation Model, travelling grate

## Introduction

Due to high CO<sub>2</sub> emissions thermal energy conversion of fossil fuels is one major reason for the greenhouse effect. Therefore, stronger efforts should be taken to establish renewable energies in the market of heat and power generation. Especially in countries like Austria, where large biomass fuel resources are available, the combustion of wood derived fuels is an important possibility of lowering CO<sub>2</sub> emissions.

Although the performance of computers is increasing, furnace design is still based on experience and empirical data in most cases. Nevertheless, Computational Fluid Dynamics (CFD) as a tool for the design and optimisation of industrial furnaces and burners, gains increasing importance. Due to the high complexity of solid biomass combustion on fixed or moving beds only little research [3, 10, 13] has been done so far to introduce CFD as a tool for the optimisation of biomass grate furnaces in order to make thermal biomass conversion units more competitive.

In the work presented the commercial CFD software FLUENT<sup>TM</sup> was evaluated, focusing on its capability of treating special problems occurring in biomass fixed bed furnaces. Furthermore, the necessity of the implementation of additional physical models as user-defined functions was investigated. CFD calculations were performed for a CFD model of a pilot-scale biomass travelling grate furnace (nominal boiler capacity 440 kW<sub>th</sub>). Moreover, a recently developed furnace with a nominal boiler capacity of 550 kW<sub>th</sub>, which can be combined with a travelling grate as well as with a horizontally moving grate, was modelled for subsequent CFD calculations concerning the optimisation of the furnace geometry (combustion chambers and secondary air nozzles). The mass and energy fluxes from the biomass fuel bed (drying, devolatilisation and heterogeneous charcoal combustion) into the gas phase, forming the boundary conditions for CFD simulations, are calculated with a simple empirically derived model based on integral balancing. This model is the subject of further development. The plausibility of calculation results was checked by hot gas FT-IR measurements and conventional flue gas measurements which took place during test runs performed at the pilot-scale travelling grate furnace under well defined conditions [6, 25].

## Mass and energy fluxes in biomass grate furnaces – calculation of boundary conditions

An empirically derived model consisting of two main parts was used for the calculation of the mass and energy fluxes from the fuel bed to the gas phase. The first part is programmed for the calculation of total mass fluxes of primary air, secondary air, recirculated flue gas and solid biomass fuel which are used as boundary conditions for subsequent CFD calculations. In order to calculate the distribution of mass fluxes from the biomass fuel bed into the gas phase along the grate, the second part of the program is needed for integral balancing. Experiments have shown a linear correlation between the individual components H<sub>2</sub>O, C, H, N and O released from the biomass fuel bed [25]. This makes the mathematical description of the fuel consumption with one leading parameter (e.g. release of C) possible, for whom a profile has to be described. This description is based on test runs performed under defined conditions at a pilot-scale grate furnace by taking and analysing samples from different parts of the fuel bed in a number of repetitions.

Conversion parameters must be given to calculate the local concentrations of different species (CH<sub>4</sub>, CO, CO<sub>2</sub>, H<sub>2</sub>, H<sub>2</sub>O, O<sub>2</sub>) in the flue gas released from the fuel bed along the grate. These conversion parameters are based on literature [11, 22] and need more detailed investigation in the near future. An estimation of the ratio between unburned and burned flue gas is also possible by comparison of the temperature profile calculated with temperature values measured using thermocouples placed above the different grate sections.

Currently, decoupling of heterogeneous biomass combustion on the grate and turbulent reacting flow of flue gas in the combustion chamber is assumed. Therefore, the influence of furnace geometry and operation conditions (radiative and convective heat transfer between flue gas and fuel bed) on chemical and physical sub-processes occurring in the biomass fuel bed cannot be taken into consideration explicitly. The present model was developed especially focusing on biomass grate furnaces with combustion chamber geometries similar to the ones shown in the section *Description of the Low-NO<sub>x</sub> biomass furnaces modelled*. For these geometries, the model is sufficiently accurate regarding its application for subsequent CFD calculations aiming at the optimisation of flue gas burnout as well as the minimisation of furnace volume.

In order to achieve a more detailed description of heterogeneous biomass combustion on the grate, the model is being developed further. The modelling parameters needed are to be determined by measurements at a specially designed lab-scale reactor with a hot gas FT-IR measurement system, which allows several flue gas components in the hot furnace (CH<sub>4</sub>, CO, CO<sub>2</sub>, H<sub>2</sub>O) to be determined in-situ.

Figure 1 to Figure 3 show different profiles of local temperature, flue gas velocity and concentration of CO in the flue gas released from the fuel bed along the grate, calculated with the empirically derived model explained.

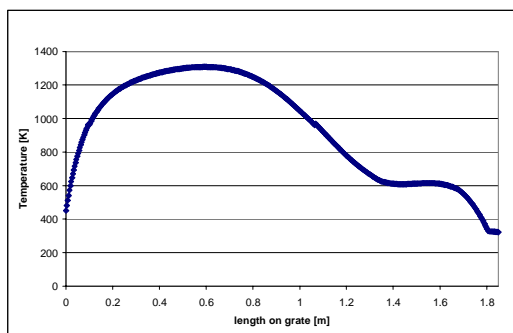


**Figure 1:** Profile of local flue gas temperature [K] along the travelling grate

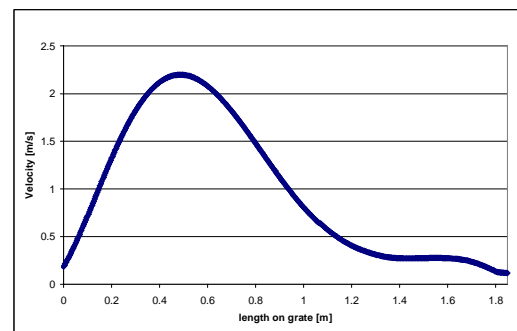


**Figure 3:** Profile of flue gas velocity [m/s] along the travelling grate

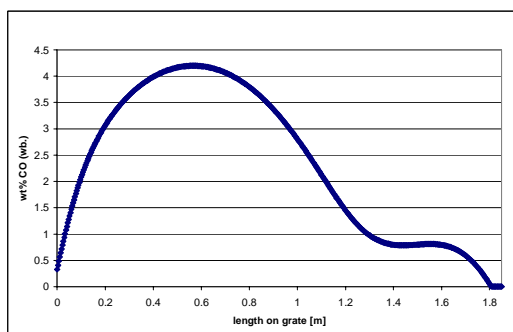


**Figure 2:** Profile of local concentration of CO in the flue gas [kg CO / kg wet flue gas] released from the fuel bed along the travelling grate

**Explanations concerning Figures 1 to 3**

grate system	travelling grate
fuel type	waste wood
water content	16 wt% H <sub>2</sub> O
primary air ratio	$\lambda_{\text{prim}} = 1.0$
flue gas recirculation ratio	0.3

## CFD modelling

### a) Common

A solver for unstructured grids (FLUENT 5) which allows to model furnaces with complex geometry and solution-adaptive grid-refinement was applied. The following numerical methods and physical models implemented in FLUENT 5 have been used (for explanations of theory see FLUENT user's guide [9]) for 3D modelling of turbulent combustion including heat transfer. The SIMPLE algorithm of the segregated solver for non-compressible and moderate compressible flows was used for pressure-velocity coupling. A second-order Upwind Scheme was applied for discretisation of convective terms of the transport equations for mass, momentum, species and energy. The Realizable k- $\epsilon$  Model used for turbulence modelling in the present work is a relatively new development and is nearly as numerically robust and CPU efficient as the Standard k- $\epsilon$  Model but provides substantial improvements for flows including rotation, strong streamline curvature and vortices (recirculation). The Discrete Ordinates Model (DOM) solving the radiative transport equation for a finite number of discrete solid angles was used for radiation modelling. The main advantage of this model is that it covers the whole range of optical thicknesses with high accuracy and it is well suitable for combustion problems.

### b) Combustion

The most important flue gas components to be considered in biomass combustion processes are  $C_mH_n$  (represented by Methane),  $H_2$ , CO,  $CO_2$ ,  $H_2O$ ,  $O_2$  and  $N_2$ . Therefore, a global reaction mechanism including CO and  $H_2$  as intermediate species should be used. Several 3-step mechanisms have been proposed in literature usually estimating the amount of  $H_2$  and  $H_2O$  formed from hydrocarbon combustion. In the present work a 3-step mechanism (see Equation 1 to 3) from literature was used in which 1.2 Mole  $H_2$  and 0.8 Mole  $H_2O$  are formed from 1 Mole  $CH_4$  [1, 2].



A multi-step Finite Rate Chemistry/Eddy Dissipation Model, which is implemented in most commercial CFD codes, was used. A mixing rate (turbulent time-scale) and an Arrhenius rate (chemical time-scale) are calculated and the smaller (limiting) value is used as the reaction rate.

In the present global mechanism the reactions described in Equation 1 and 3 are assumed to be controlled by the turbulent mixing rate. The reaction described in Equation 2 (consumption of CO) is determined by the lower (limiting) rate of either reaction kinetics or turbulent mixing. All reactions are assumed to be irreversible.

The Eddy Dissipation Model by Magnussen and Hjertager [19] is reasonably accurate for most practical applications, numerically robust and applicable to premixed, non-premixed and partially premixed combustion but has several disadvantages, like

- unreliability of calculated results when time-scales of turbulent mixing and reaction kinetics are similar ( $Da \approx 1$ ),

- phenomena like ignition and extinction, which depend on reaction kinetics, cannot be described properly,
- intermediate species (radicals) and dissociation effects are disregarded, which leads to an over-prediction of local flame temperature,
- the influence of turbulent fluctuations on reaction kinetics is not accounted for,
- the empirical constants of the mixing rates for the reactants and products are not universally valid and therefore should be calibrated for different types of combustible flows.

An important consequence of the fact that strong coupling between turbulence and multi-step chemistry cannot be described properly is that the Eddy Dissipation Model is not well suited for the modelling of NO<sub>x</sub> chemistry.

The limitations due to the bottlenecks described concerning practical applications and, as a consequence, possible improvements of the Eddy Dissipation Model included in Fluent™ will be discussed in the section *Modelling of Low-NO<sub>x</sub> biomass grate furnaces - evaluation of the CFD code FLUENT™*.

### c) Euler-Lagrange particle tracing

A particle tracing procedure was used to calculate erosion rates and residence time distributions of the flue gas. In order to calculate particle trajectories the force balance on a fly ash particle (see Equation 4), written in a Lagrangian reference frame, is integrated.

$$\frac{du_p}{dt} = F_D(u - u_p) + g_x(\rho_p - \rho) / \rho_p + F_x \quad \text{Equation 4}$$

The term on the left side of Equation 4 is the particle inertia, the first term on the right side is the drag force per unit particle mass, the second term includes the force of gravity on the particle,  $F_x$  includes additional forces, such as forces observed in rotating flow domains, thermophoretic forces as well as the impact of Brownian motion for sub-micron particles.

The turbulent dispersion of the particles is calculated using a stochastic particle tracing procedure including the instantaneous value  $u$  of the gas flow velocity, calculated from mean velocity  $\bar{u}$  and velocity fluctuation  $u'$  (see Equation 5).

$$u = \bar{u} + u' \quad \text{Equation 5}$$

The calculation of residence time requires the distributions of the virtual tracer particles moving with the flue gas to be defined. The trajectories of tracer particles are calculated using the mean fluid phase velocity  $\bar{u}$ .

Particle tracing could also be applied to the prediction of fly ash deposition and slagging films. For this purpose, the user must implement his own sub-models as user-defined functions [8].

### Description of the Low-NO<sub>x</sub> biomass furnaces modelled

Two different biomass low-NO<sub>x</sub> grate furnaces were used for modelling. Both furnaces consist of a combustion chamber (modelled part) which is combined with two different grate systems (a travelling grate in one case and a horizontally moving grate in the other). Both were designed and constructed by the biomass furnace and boiler manufacturer MAWERA

(Hard, Austria) in co-operation with BIOS Consulting, Graz, and the Institute of Chemical Engineering Fundamentals and Plant Engineering at the Technical University Graz, Austria.

Low NO<sub>x</sub> combustion chambers are divided into primary and secondary combustion zones. The primary combustion zone is designed as an air lean hot reduction zone with sufficient residence time for the flue gas to decrease NO<sub>x</sub> emissions by primary measures. The secondary combustion zone is designed as an air rich burnout zone. Flue gas recirculation is used for temperature control. The amount of excess oxygen (secondary air) is controlled by the CO concentration in the flue gas at boiler outlet.

Furnace geometry No. 1 is part of a pilot-scale plant with a nominal boiler capacity of 440 kW<sub>th</sub>. The furnace (Figure 4) is divided into three horizontally arranged combustion chambers. The first chamber above the grate and the second chamber are forming the air lean primary combustion zone (reduction zone). The tertiary chamber is designed as a secondary combustion zone for the purpose of sufficient flue gas burnout.

Furnace geometry No. 2 (Figure 5) is part of a newly developed furnace with a nominal boiler capacity of 550 kW<sub>th</sub> and consists of a horizontal combustion chamber above the grate and three vertical combustion chambers.

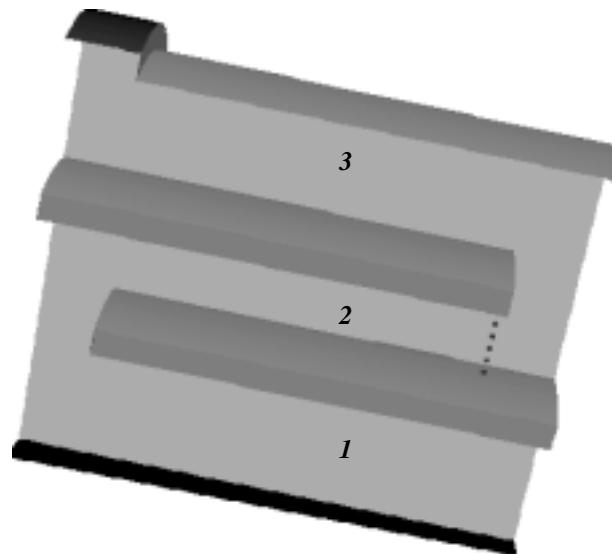


**Figure 4:** Modelled part of the combustion chamber No. 1 (Low-NO<sub>x</sub> furnace, nominal boiler capacity 440 kW<sub>th</sub>)

**Explanations**

- 1.....primary combustion chamber above the grate (primary combustion zone), release of flue gas from the fuel bed, primary air supply and recirculated flue gas under the grate
  - 2.....secondary combustion chamber (primary combustion zone) designed as air lean hot reduction zone
  - 3.....tertiary combustion chamber (secondary combustion zone) designed for efficient flue gas burnout after air injection
- between 2 and 3.....nozzles for secondary air supply and flue gas recirculation

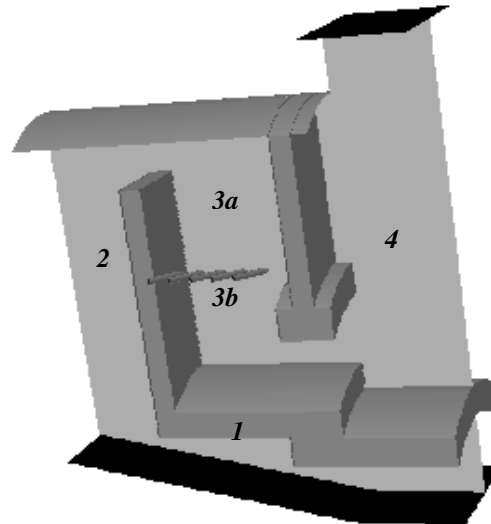


**Figure 5:** Modelled part of the combustion chamber No. 2 (Low-NO<sub>x</sub> furnace, nominal boiler capacity 550 kW<sub>th</sub>)

**Explanations**

- 1.....Horizontal chamber above the grate (primary combustion zone), release of flue gas from the fuel bed, primary air supply and flue gas recirculation under the grate
- 2.....first vertical chamber (primary combustion zone)
- 3a.....second vertical chamber (primary combustion zone)
- 3b.....second vertical chamber (secondary combustion zone)
- between 3a and 3b.....nozzles for secondary air supply and flue gas recirculation
- 4.....third vertical chamber (secondary combustion zone)

Two grate systems can be applied to both furnace geometries. The travelling grate is mainly used for homogeneous and dry biomass fuels, especially waste wood. Advantages of the travelling grate are the robustness against slagging and low fly ash emissions. The travelling grate needs a minimum primary air ratio of about  $\lambda_{prim} = 1.0$  to achieve a sufficient charcoal burnout.

The horizontally moving grate is designed for a broader biomass fuel assortment and is especially suitable for heterogeneous and wet biomass fuels. This grate technology allows primary air ratios of between  $\lambda_{prim} = 0.7 - 0.8$  to achieve a complete charcoal burnout. The reason for the lower possible primary air ratio is that the fuel bed gets mixed by the grate movements, which is not the case for the travelling grate.

## **Modelling of Low-NO<sub>x</sub> biomass grate furnaces - evaluation of the CFD code FLUENT™**

### **a) Combustion model**

As already mentioned, the Eddy Dissipation Model implemented in most commercial CFD codes is simple, numerically robust and universally applicable but also contains many weak points. One main disadvantage is the fact that the empirical parameters used for the calculations of the mixing rate are not universally valid and have to be modified for different applications (time and length scales). Several values concerning the mixing parameter for the reactants have been discussed in literature [14, 19, 23, 24]. Magnussen and Hjertager proposed a value of 4.0 in their original work. For swirling coal flames, Visser found a value of 0.5 - 0.7 to give the best results for flame prediction. According to the literature data proposed and CO measurements performed at the modelled pilot-scale plant, values between

0.6 and 1.0 show the best agreement between CO concentrations calculated with the global 3-step mechanism and control measurements and are thus best suited for biomass grate furnaces. Figure 6 shows local CO concentrations in the biomass grate furnace No. 1 calculated with different mixing parameter values. A value of 4.0 underpredicts the local CO concentrations, a value of 0.6 slightly overpredicts local CO concentrations according to results obtained with a newly developed FT-IR (Fourier-transformed infrared spectroscopy) hot gas in-situ measurement technique (measurements at different sections in the hot furnace) and a conventional CO measurement technique (measurements at boiler outlet). A value of 1.0 used in another case study gave an agreement of reasonable accuracy between CFD calculations and measurements. For the case studies described in this paper, a value of 0.6 was used to design the furnace geometry in order to ensure compliance with emission limits. Therefore, the local CO concentrations calculated should be regarded as trends and not as accurate values.

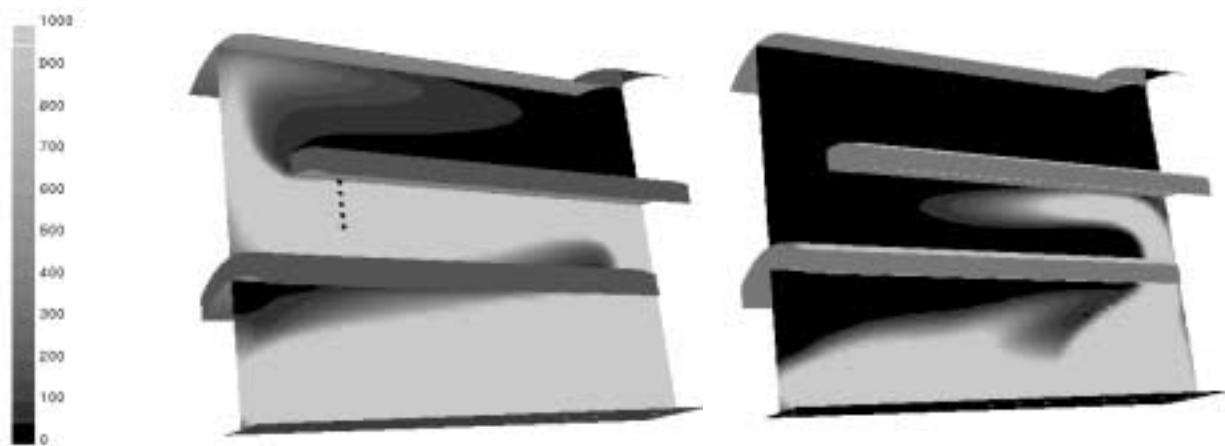


**Figure 6:** Contours of local CO concentrations [vol-ppm] in a biomass grate furnace calculated with different values of the mixing constant for reactants

**Explanations**

Left.....local CO concentrations using the mixing parameter according to Visser: 0.6

Right.....local CO concentrations using the mixing parameter according to Magnussen and Hjertager: 4.0

Further weaknesses of the Eddy Dissipation Model used for these calculations are the limitations regarding strong coupling between turbulence and reaction kinetics (e.g. NO<sub>x</sub> kinetics). In order to improve flame prediction, an advanced Eddy Dissipation Concept [5, 12, 14, 15, 16, 17, 18, 20, 21] which treats the fine structures of the eddy dissipation cascade as perfectly stirred reactors and represents a more general formulation of the Eddy Dissipation Model, is currently being implemented. Additionally, a global reaction mechanism considering the most important species for biomass combustion and validated for conditions prevailing in biomass grate furnaces will be implemented. The estimated ratio of the locally formed concentrations of H<sub>2</sub> and H<sub>2</sub>O will be abandoned and a more fundamental formulation based on a model proposed in literature [2, 18] will be implemented in the calculation routines. A model for local flame extinction [4] and a NO<sub>x</sub> post-processor [15] will also be combined with the Eddy Dissipation Concept.

## b) Erosion

Optimisation of biomass grate furnaces should not only consider a reduction of furnace volume and emissions, but must also include the calculation of total pressure loss in the combustion chamber for air supply / flue gas recirculation, and the prediction of fly ash precipitation, erosion and slagging in the furnace in order to additionally minimise investment and operating cost. In this paper an investigation of FLUENT™ regarding its capacity to

predict erosion was performed. Erosion rates at furnace walls are formulated according to Equation 6.

$$R_{erosion} = \sum_{p=1}^{N_{particles}} \frac{\dot{m}_p \times f(\alpha) \times f(d_p) \times u_p^{f(u_p)}}{A_{face}} \quad \text{Equation 6}$$

The rate of erosion  $R_{erosion}$  per unit furnace wall  $A_{face}$  is a function of particle mass stream  $\dot{m}_p$ , and the dimensionless functions  $f$  of impact angle  $\alpha$ , impact particle velocity  $u_p$  and particle diameter  $d_p$ . In order to take into account the material dependence of the erosion rate, a constant value should be introduced as a correction factor. In the case study performed the calculated rate of erosion is assumed only to be a function of the particle mass stream and impact angle (only the shear effect of the particles is considered; linear interpolation of the function between the values: impact angle  $\alpha=0^\circ$ :  $f(\alpha)=1.0$  and impact angle  $\alpha=90^\circ$ :  $f(\alpha)=0$ ). Moreover, the calculations were not based on a certain fly ash particle size distribution but on the mean diameter of the coarse fly ash particles in the flue gas.

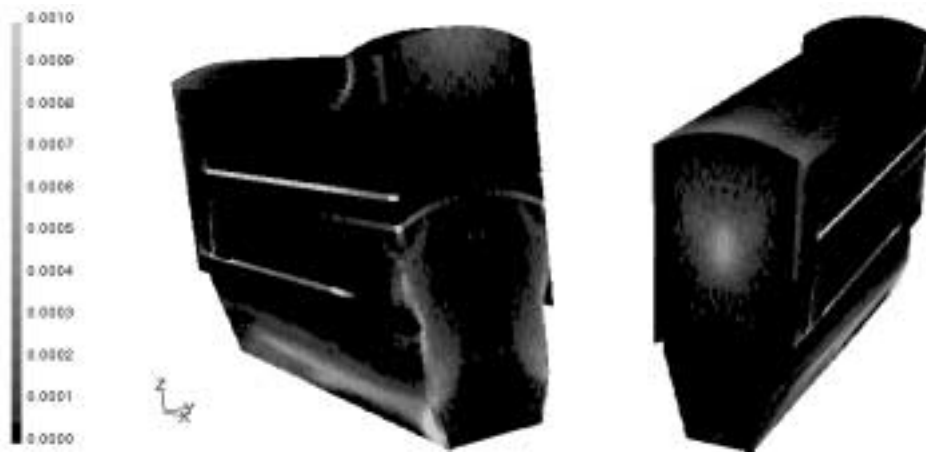


**Figure 7:** Calculated erosion rates [kg/m<sup>2</sup>s] for the combustion chamber walls

*Explanations*

Input parameters: flue gas dust load = 500 mg/Nm<sup>3</sup>; fly ash mean particle diameter = 100 μm; fly ash particle density = 2000 kg/m<sup>3</sup>; 1/3 of fly ash particle mass emitted from the third quarter of grate length measured from fuel supply, 2/3 of fly ash particle mass emitted from the fourth quarter of grate length measured from fuel supply.

Left.....Erosion rates on front and left furnace walls - seen from the fuel supply side  
 Right.....Erosion rates on back and right furnace walls - seen from the ash discharge side

The calculation results achieved show a good qualitative agreement with erosion observed in the combustion chamber of the biomass grate furnace No.1. In Figure 7 it can be seen that abrasion of combustion chamber material is especially strong at the regions of transition between the combustion chambers. Additional test runs have to be performed in order to obtain more detailed and qualitative information about erosion occurring in the furnace and more comprehensive data concerning the parameters in Equation 6.

**c) Residence time distribution**

Up to now, furnace design regarding flue gas burnout and NO<sub>x</sub> reduction by primary measures was usually based on the mean residence time of the flue gas in the furnace based on the formula “residence time = volume flow / furnace volume”, which disregards dead zones in the combustion chamber.

A particle tracing procedure was used in the CFD calculations to determine “real” mean residence times of the flue gas in the furnace. For this purpose “tracer particles” which move with the fluid are injected into the flue gas stream leaving the fuel bed.

Moreover, the residence time distribution calculated offers additional information concerning NO<sub>x</sub> reduction technologies. Residence time histograms achieved with CFD calculation form a valuable basis for comparison with the residence time distributions of ideal reactor models, which allow the detailed kinetic investigation of gas-phase NO<sub>x</sub> formation reactions (plug flow reactor, perfectly stirred reactor or combinations). Consequently, the reactor models can be better adjusted to the furnace conditions. The results achieved from such models considering NO<sub>x</sub> formation reactions in detail can then complement the outcome of CFD calculations obtained with NO<sub>x</sub> postprocessor routines which take flow conditions into account. The combination of both measures forms an improved basis for the development and evaluation of NO<sub>x</sub> reduction technologies based on primary measures.

Figure 8 shows examples of residence time distributions for the flue gas released from the biomass fuel bed in the primary combustion zone for two variations of furnace No. 2. Residence time distributions (as well as mean residence time and minimum residence time) showed were used in order to assess the NO<sub>x</sub> reduction potential of the furnace variations.

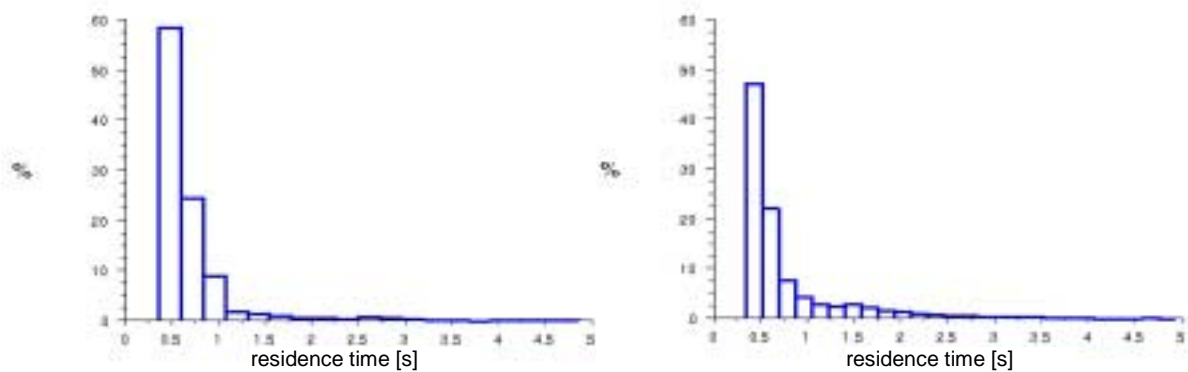


**Figure 8:** Residence time distribution of the flue gas released from the biomass fuel bed in the primary combustion zone for two variations of furnace geometry No. 2.

**Explanations**

Left diagram.....histogram of the residence time distribution of the flue gas released from biomass fuel bed in primary combustion zone for the reference case (minimum value 0,37 s, mean value 0.71 s, standard deviation 0.52 s)

Right diagram.....histogram of the residence time distribution of the flue gas released from biomass fuel bed in primary combustion zone for geometric variation No. 1 – see following chapter (minimum value 0.35s, mean value 0.81 s, standard deviation 0.72s)

**Optimisation of furnace geometry regarding flue gas burnout - a case study**

A case study regarding optimisation of flue gas burnout and furnace volume was performed for furnace geometry No. 2. The results presented are aimed at improving an existing type of biomass furnace rather than developing an optimised biomass low NO<sub>x</sub> furnace from scratch. This optimisation took place in two steps. At first the combustion chambers are modified in order to improve utilisation of the furnace volume and increase the turbulent mixing of combustible flue gas components and oxygen (air). In a second step the arrangement of the secondary air nozzles was varied, taking the simulation case with the lowest CO emissions achieved from the first step as a basis and focusing on a further improvement of flue gas burnout by increasing the mixing of secondary air and flue gas. The operating data used for this case study are shown in Table 1. Values of local CO emissions and temperatures calculated should be considered as trends and not as accurate values.

**Table 1:** Operating data used for simulating combustion in biomass grate furnace No. 2

parameter	value	unit
grate system	travelling grate	
nominal boiler capacity	550	kW <sub>th</sub>
primary air ratio	1.0	
total air ratio	1.6	
recirculation ratio	0.3	(mass stream of flue gas recirculated / mass stream of flue gas in the combustion chamber)
fuel type	waste wood	
water content	16	wt% (w.b.)

### a) Optimisation of the combustion chamber geometry

Figure 9 shows the visualisation of different flow properties in biomass grate furnace No. 2. The mean CO emissions as the leading parameter for calculated flue gas burnout at the furnace outlet amount to about 20 vol-ppm. This result shows that mixing of combustible flue gas components and air in the furnace geometry is good and almost complete burnout is achieved. Consequently, the aim of furnace geometry optimisation in this case focuses on reducing the height of the combustion chambers in order to minimise plant costs or to increase thermal efficiency by lowering the excess air needed (further improvement of mixing conditions).

In the present case study the majority of combustible flue gas components is already burned in the primary combustion chamber due to the good turbulent mixing achieved by a strong curvature of the flue gas stream and narrow passages in the furnace. This fact causes relatively high local temperature peaks in the primary combustion zone (1,270°C in the present case). The temperatures occurring in the furnace have to be controlled in order to prevent slagging and hard deposit formation. Temperature control can be achieved by flue gas recirculation. An injection of flue gas at the transition between the horizontal combustion chamber and the first vertical combustion chamber homogenises the flue gas composition in the primary combustion zone by turbulent mixing and therefore lowers temperature peaks and destroys CO strains. Moreover, the maximum total pressure of the flue gas in the furnace should be calculated in order to design flue gas and air fans properly and to estimate the corresponding operating costs. For the reference case a total pressure loss of about 300 Pascal was calculated between secondary air nozzles and furnace outlet.

Based on the reference case the furnace geometry was varied to achieve a reduction of furnace volume. Two variations were found to be optimal for different reasons. In the first geometric variation the furnace height was reduced by one chamotte brick. Furthermore, the step in the combustion chamber was moved to the left to increase flue gas residence time in the secondary combustion zone as a consequence of a better utilisation of the furnace volume after the step (compare geometries shown in Fig. 9 and Fig. 10). Further design modifications include a narrower second combustion chamber, a wider third combustion chamber, lower secondary air nozzles and a lower transition between third and fourth combustion chamber in order to achieve a higher mixing rate of flue gas and air and increased residence time in the primary combustion zone.

The CO emissions calculated for geometric variation No. 1 are even slightly lower than emissions calculated for the reference case. The temperature peak in the primary combustion zone is only a few degrees higher than in the reference case. Total pressure loss between the

secondary air nozzles and the transition to the heat exchanger of the furnace increased by about 5 percent. Variation No. 1 is recommended if the major goal is a minimisation of excess oxygen in the flue gas combined with moderate savings in investment cost.

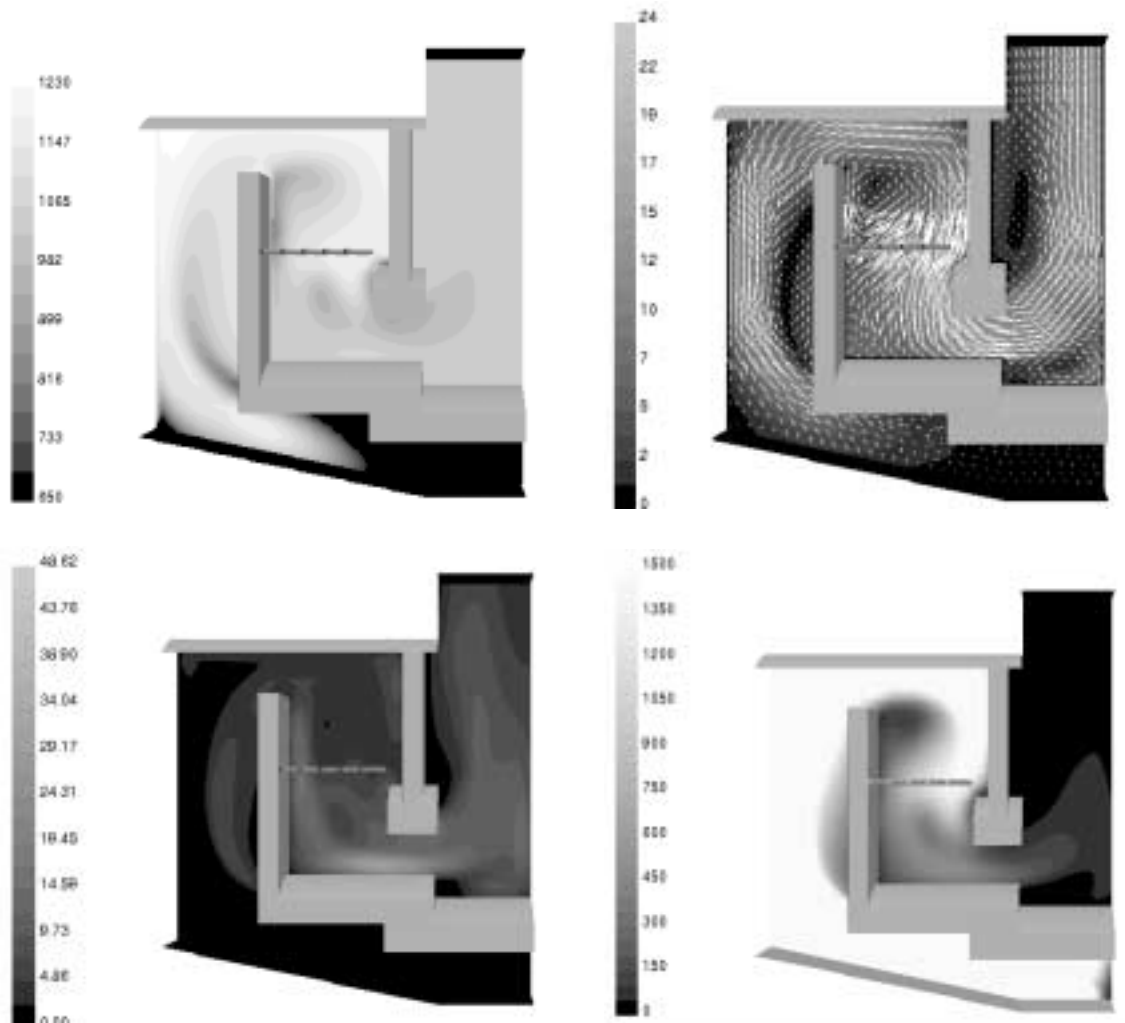


**Figure 9:** CFD modelling results for biomass grate furnace No. 2 – reference case

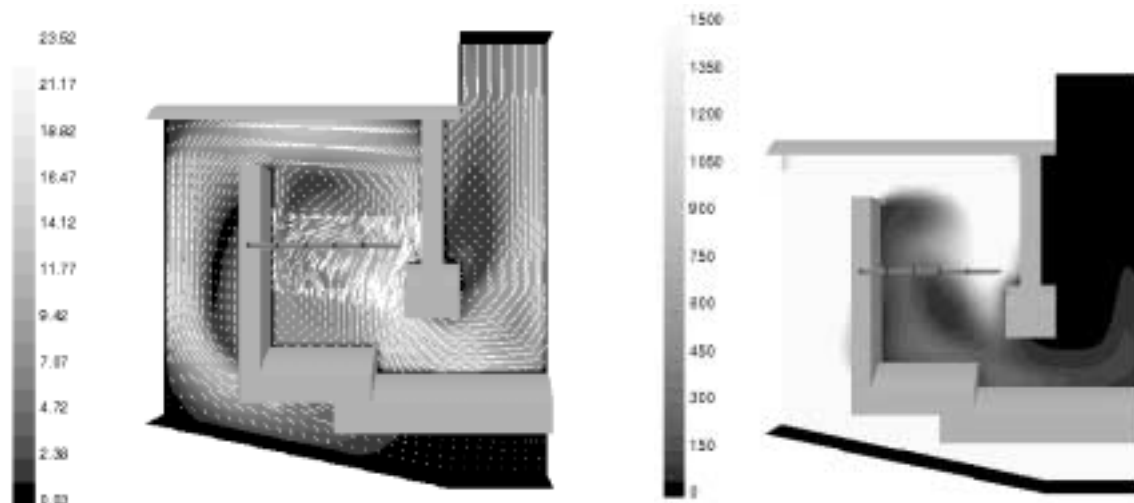
**Explanations**

- Top left.....distribution of flue gas temperature [°C]
- Top right.....distribution of flue gas velocity [m/s] combined with vector plots of flue gas velocity
- Bottom left.....distribution of turbulent kinetic energy [m<sup>2</sup>/s<sup>2</sup>]
- Bottom right.....distribution of CO concentrations [vol-ppm]

In the second variation the furnace height was reduced by two chamotte bricks with the same furnace design as variation No. 1. Additionally, the secondary air nozzles were moved downstream in order to partially compensate for the decrease of residence time in the air lean primary combustion zone with regard to NO<sub>x</sub> emissions due to the reduction of furnace height.

The CO emissions calculated for geometric variation No. 2 are about 1.5 times higher than emissions calculated for the reference case. This is due to the significant further reduction in furnace volume and the positioning of the secondary air nozzles. The nozzles are placed low, which reduces the residence time of the flue gas required to achieve a complete burnout. Nevertheless, the CO emissions for variation No. 2 are quite satisfactory, taking into consideration the low values of the mixing parameters used in the Eddy Dissipation Model, which result in a slight overprediction of CO emissions for biomass grate furnaces and can be

regarded as an additional safety margin. The total pressure drop calculated is nearly the same as for the reference case. The temperature peak is also located in the same region and shows about the same value as calculated for the reference case and variation No. 1. Consequently,



variation No. 2 allows for an additional reduction of investment costs (furnace volume).

**Figure 10:** CFD modelling results for biomass grate furnace No. 2 - variation No. 1

*Explanations*

Left.....distribution of flue gas velocity [m/s] combined with vector plots of flue gas velocity  
Right.....distribution of CO concentrations [vol-ppm]

## b) Optimisation of the secondary air nozzles

Besides the variation of furnace geometry, several geometric variations of the secondary air nozzles were investigated in order to optimise mixing conditions and flue gas burnout. The optimal variation results in comparison with the reference case are presented. Furthermore, relevant influencing parameters for a good turbulent mixing of unburned flue gas and secondary air and guidelines for the optimisation of the secondary air nozzles are outlined.

The design of combustion chambers and secondary air nozzles of geometric variation No. 1 (biomass grate furnace No.2) is taken as reference case. Simulation results are shown in Figure 11. Concentration profiles represented in three cross-sections at the level of the nozzles and below show a CO-rich core flow next to the furnace wall between third and fourth combustion chamber. This is a result of the asymmetric arrangement of the secondary air nozzles, which produces a weak swirl in the region where the major part of the flue gas stream passes the secondary air nozzles, and a stronger swirl next to the furnace wall (see Figure 11). Moreover, the momentum of secondary air is relatively weak due to the high number of secondary air nozzles. Additionally, the mixing effect achieved by the secondary air nozzles next to the furnace wall between second and third combustion chamber is relatively small due to the locally low flue gas flow.

Due to these findings, the simulated geometric variations aimed at an improved turbulent and convective mixing of flue gas and air by reducing the number, and optionally the diameter, of the secondary air nozzles. Major efforts were focused on achieving a high stagnation momentum of secondary air, on placing the nozzles outside regions of low flue gas streams and on producing a swirling flow. Several geometric variations of the nozzles were tested in order to fulfil these objectives.

Two different properties of the flow pattern of the best simulation case are shown in Figure 12. The CO emissions as the key parameter for flue gas burnout at the furnace outlet were significantly decreased in comparison to the reference case (to about a third). This is primarily

due to the arrangement of the secondary air nozzles selected. Moreover, the number of nozzles was reduced in order to increase the stagnation momentum (nozzles located in regions of low flue gas flow were removed). The secondary air nozzles on both sides of the combustion chamber were arranged in horizontal rows symmetrically to the central plane and inclined at an angle of 45° to the furnace wall. An improved mixing of unburned flue gas and air by a higher turbulence and a better penetration with secondary air due to a higher momentum of secondary air and the induction of two swirls covering the whole furnace cross-section could be achieved, which resulted in earlier CO burnout. Due to these improved mixing conditions, a total pressure loss of secondary air exceeding the corresponding value of the reference case by about 80 percent must be considered for air and flue gas fan design.

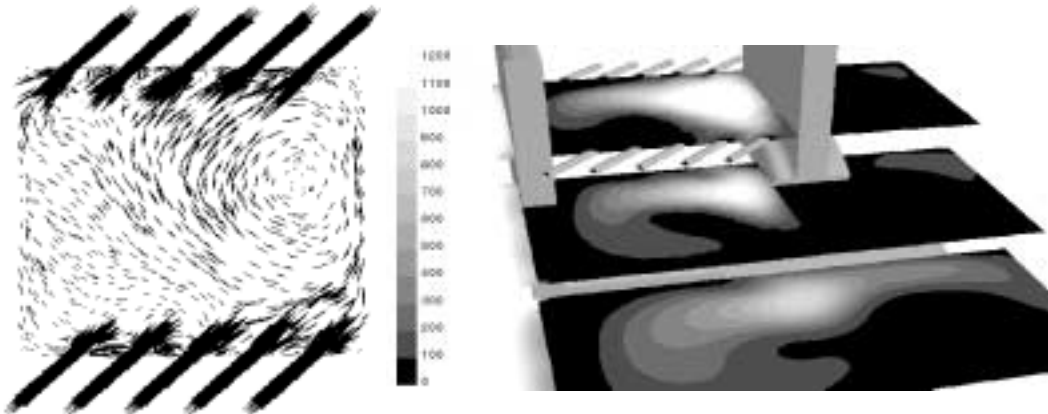


**Figure 11:** Flue gas velocity as well as CO distribution in different cross-sections near secondary air injection – reference case for secondary air nozzle geometry

**Explanations**

secondary air nozzles in biomass furnace No. 2, variation No. 1 (see Figure 10)

Left.....vector plots of flue gas and secondary air velocity in the cross-section of the furnace at the level of the nozzles

Right.....distribution of CO concentrations [vol-ppm] in three different cross-sections of the furnace (section at the level of the secondary air nozzles; section 200 mm below; section 400 mm below)

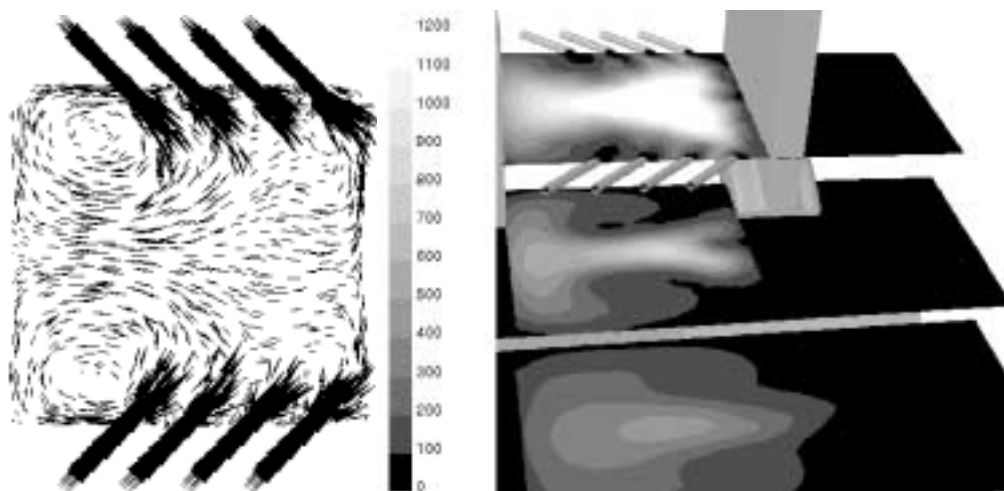


**Figure 12:** Flue gas velocity as well as CO distribution in different cross-sections near secondary air injection – optimised design of secondary air nozzles

**Explanations**

Left.....vector plots of flue gas and secondary air velocity in the cross-section of the furnace at the level of the nozzles

Right.....distribution of CO concentrations [vol-ppm] in three different cross-sections of the furnace (section at the level of the secondary air nozzles; section 200 mm below; section 400 mm below)

As mentioned, the calculated CO emissions should be regarded as trends and are far below the emission limits, even for the reference case. Therefore, a lowering of CO emissions is not of primary interest for the case study presented but should be considered as an indicator for a possible reduction of the amount of excess air. In order to obtain more detailed information about the total air ratio within reach further investigations should be performed.

This improved geometry of secondary air nozzles can be generally recommended for biomass furnace geometries with a rectangular cross-section and similar local flow conditions as in the simulated geometric case study.

## **Conclusions**

The application of the CFD software FLUENT™ for the optimisation of biomass grate furnaces revealed a great potential for improvements in different ways. Even with isothermal flow calculations the furnace volume can be minimised by avoiding dead zones. Erosion can be reduced by estimating the erosion rates with a particle tracing procedure. The implementation of additional sub-models allows for the prediction of ash deposition and slagging on furnace walls. Total pressure loss in combustion chambers can be calculated in order to dimension flue gas and air fans as well as to calculate the corresponding operating costs.

The Eddy Dissipation Model used for combustion simulation is reasonably accurate for most industrial flow problems but cannot properly describe strong coupling between turbulence and multi-step chemistry (e.g. calculation of NO<sub>x</sub> emissions). Therefore, an advanced Eddy Dissipation Concept, which treats the fine structures of the eddy dissipation cascade as perfectly stirred reactors and represents a more general formulation of the Eddy Dissipation Model, is being implemented.

Moreover, the case study performed should be regarded as an improvement of an existing type of biomass furnace rather than a completely new development of an optimised biomass Low-NO<sub>x</sub> furnace. The simulation results revealed a considerable potential for improving mixing conditions and CO burnout through modifications of furnace geometry and secondary air nozzles. Furthermore, the optimised secondary air nozzles can be generally recommended for biomass furnace geometries with a rectangular cross-section and local flow conditions similar to the simulated geometric case study. The calculated CO concentrations should be considered as trends and are well below the emission limits for all calculated variations including the reference case. Therefore, a lowering of CO emissions is not of interest for the defined operating conditions but should be considered as an indicator for a possible reduction of the amount of excess air in order to increase the thermal efficiency of the furnace. In order to obtain more detailed information about the total air ratio within reach further investigations have to be performed, but a considerable potential is obvious.

Taking the results already achieved into consideration it can be stated that CFD calculations generally represent an efficient tool for the technological and economic optimisation of biomass fixed-bed combustion systems and provide an important basis for other post-processing calculation routines (e.g. chemical kinetic calculations, ash deposit calculations).

## **Acknowledgements**

This work was supported by the Austrian Industrial Research Promotion Fund (FFF) and the Company MAWERA Wood Combustion Systems in Austria.

## Nomenclature

$\rho$	gas density [kg/m <sup>3</sup> ]	$f(d_p)$	function of particle diameter [-]
$\lambda$	stoichiometric air ratio [-]	$F_D$	drag force per unit particle mass [1/s]
$\lambda_{\text{prim}}$	primary air ratio [-]	$F_x$	additional particle forces [m/s <sup>2</sup> ]
$\rho_p$	particle density [kg/m <sup>3</sup> ]	$g_x$	gravity force [m/s <sup>2</sup> ]
$A_{\text{face}}$	combustion chamber surface [m <sup>2</sup> ]	$R_{\text{erosion}}$	rate of erosion [kg/m <sup>2</sup> s]
$\dot{m}_p$	particle mass stream [kg/s]	$u$	flue gas velocity [m/s]
$\alpha$	particle impact angle [rad]	$u_p$	particle velocity [m/s]
$d_p$	particle diameter [m]		
$f(\alpha)$	function of particle impact angle [-]		
$f(u_p)$	function of particle velocity [-]		

## Literature

- 1 ABDALLA A.Y., BRADELY D., CHIN S.B. & LAM C., 1983: Global reaction schemes for hydrocarbon combustion, *Oxidation Communications*, Vol. 4, No. 1-4, pp. 113-130
- 2 BRINK, A., KILPINEN, P., HUPA, M., KJÄLDMAN, L., JÄÄSKELÄINEN, K., 1995: Fuel Chemistry for Computational Fluid Dynamics, 2<sup>nd</sup> Colloquium on Process Simulation, Espoo, Finland, 6.-8. June, 1995
- 3 BRUCH, C., NUSSBAUMER, T., 1998: CFD Modelling of Wood Furnaces. In: Proceedings of the 10th European Bioenergy Conference, June 1998, Würzburg, Germany, C.A.R.M.E.N. (ed), Rimpf, Germany
- 4 BYGGSTOYL, S., MAGNUSSEN, B. F., 1985: A model for flame extinction in turbulent flow, *Turbulent Shear Flows 4*, edited by L. J. S. Bradbury et al., Springer Verlag, Berlin, 1985, pp. 381-395
- 5 ERTESVAG, I. S., MAGNUSSEN, B.F., 1997: The Eddy Dissipation turbulence energy cascade model, SINTEF Energy, report no. STF84 A97501, ISBN 82-595-9100-6
- 6 FLECKL, T., OBERNBERGER, I. 2000: Combustion diagnostics at a biomass-fired grate furnace using FT-IR absorption spectroscopy for hot gas measurements. In: Proceedings of the 5<sup>th</sup> International Conference of Industrial Furnaces and Boilers, April 2000, Porto, Portugal
- 7 FLUENT Deutschland GmbH (Ed.), 1998: Tagungsband des Fluent Anwendertreffens, 21.-22. September 1998, Darmstadt, Deutschland
- 8 FLUENT Deutschland GmbH (Ed.), 1999: Tagungsband des Fluent Anwendertreffens, 20.-21. September 1998, Mannheim/Viernheim, Deutschland
- 9 FLUENT Inc., 1998: FLUENT 5 User's Guide Volume 1-4, Lebanon, USA
- 10 GRISELIN, Nicolas, BAI, Xue-Song, FUCHS, Laszlo, 1999: Tracking of particles in a biomass furnace, In: Proceedings of the 2nd Olle Lindström Symposium on Renewable Energy, Bioenergy, Royal Institute of Technology (Ed.), Stockholm, Sweden
- 11 KELLER, R., 1994: Primärmaßnahmen zur NO<sub>x</sub> Minderung bei der Holverbrennung mit dem Schwerpunkt Luftstufung, Forschungsbericht Nr. 18 (1994) Laboratory for energy systems (Ed.), ETH Zürich, Switzerland.
- 12 KJÄLDMAN, Lars, 1993: Numerical simulation of combustion and nitrogen pollutants in furnaces, VTT Publications 159, ISBN 951-38-4397-1
- 13 LINDSJO, H., BAI, X.S, FUCHS, L., 1997: Numerical and Experimental Studies of NO<sub>x</sub> Emissions in a Biomass Furnace, In: Proceedings of the 4<sup>th</sup> Int. Conference on Technologie and Combustion for a Clean Environment, Lisbon, Portugal
- 14 MAGEL, H. C. SCHNEIDER, R, RISIO, B., SCHNELL, U., HEIN, K.R.G, 1995: Numerical Simulation of Utility Boilers with Advanced Combustion Technologies. In: Proceedings of the 8<sup>th</sup> International Symposium on Transport Phenomena in Combustion, San Francisco
- 15 MAGEL, H. C., GREUL, U., SCHNELL, U., SPLIETHOFF, H., HEIN, K.R.G., 1996: NO<sub>x</sub>-Reduction with Staged Combustion – Comparison of experimental and Modelling Results. In: Proceedings of the Joint Meeting of the Portuguese, British, Spanish and Swedish Section of the Combustion Institute, Madeira, 1996
- 16 MAGEL, H. C., SCHNELL, U., HEIN, K.R.G., 1996: Modelling of Hydrocarbon and Nitrogen Chemistry in Turbulent Combustor Flows using Detailed Reaction Mechanisms. In: Proceedings of the 3<sup>rd</sup> Workshop on Modelling of Chemical Reaction Systems, Heidelberg

- 17 MAGEL, H. C., SCHNELL, U., HEIN, K.R.G.: Simulation of Detailed Chemistry in a Turbulent Combustor Flow. In: Proceedings of the 26<sup>th</sup> Symposium (International) on Combustion, The Combustion Institute (Ed.), Pittsburgh, USA, ISSN 0082-0784
- 18 MAGEL, H.C., 1997: Simulation chemischer Reaktionskinetik in turbulenten Flammen mit detaillierten und globalen Mechanismen, VDI-Fortschrittsberichte, Reihe 6: Energieerzeugung, Nr. 377, ISBN 3-18-337706-3
- 19 MAGNUSSEN, B. F., HJERTAGER, B. H., 1976: On mathematical models of turbulent combustion with special emphasis on soot formation and combustion. In: Proceedings of the 16<sup>th</sup> International Symposium on Combustion, The Combustion Institute (Ed.), Pittsburgh, USA, ISSN 0082-0784
- 20 RASMUSSEN N. B. K., MYKEN A. N., 1993: comparison/verification of advanced numerical tools for flow calculations, report, Danish Gas Technology Centre (Ed.), ISBN 87-7795-025-9
- 21 RASMUSSEN, N.B.K., MYKEN, A.N., 1994: The Eddy Dissipation Kinetic (EDK) Model for Turbulent Reactioning Flow and Numerical Implementation. In: Proceedings of the 25<sup>th</sup> International Symposium on Combustion, The University of California, Irvine, July 31 – August 5, 1994, The Combustion Institute (Ed.), Pittsburgh, USA, ISSN 0082-0784
- 22 SKREIBERG, Ø., 1997: Theoretical and Experimental Studies on Emissions From Wood Combustion, ITEV Report 97:03, ISBN 82-471-0166-1, The Norwegian University of Science and Technology, Trondheim, Norway.
- 23 VISSER B. M., 1991: Mathematical Modelling of swirling pulverised coal flames, Ph.D. thesis TU Delft
- 24 VISSER, B. M., WEBER, R., 1991: Mathematical modelling of swirl-stabilised pulverised coal flames of thermal input in the range 200 kW to 54 MW. In: Proceedings of the 15. Deutscher Flammentag, VDI Bericht Nr. 922, VDI-GET (Ed.), ISBN 3-18-090922-6
- 25 WEISSINGER, A., OBERNBERGER, I., 1997: NO<sub>x</sub> reduction by primary measures on a travelling-grate furnace for biomass fuels and waste wood. In: Proceedings of the 4<sup>th</sup> Biomass Conference of the Americas, September 1999, Oakland, USA, Ralph P. Overend and Esteban Chornet (Ed.), ISBN 0 08 043019 8